

MMSE Channel Estimation for Two-Port Demodulation Reference Signals in New Radio

Dejin Kong, Xiang-Gen Xia, *Fellow, IEEE*, Pei Liu, and Qibiao Zhu

Abstract

Two-port demodulation reference signals (DMRS) have been employed in new radio (NR) recently. In this paper, we firstly propose a minimum mean square error (MMSE) scheme with full priori knowledge (F-MMSE) to achieve the channel estimation of two-port DMRS in NR. When the two ports are assigned to different users, the full priori knowledge of two ports is not easy to be obtained for one user. Then, we present a MMSE scheme with partial priori knowledge (P-MMSE). Finally, numerical results show that the proposed schemes achieve satisfactory channel estimation performance. Moreover, for both mean square error and bit error ratio metrics, the proposed schemes can achieve better performance compared with the classical discrete Fourier transform based channel estimation. Particularly, P-MMSE scheme delivers almost the same performance compared with F-MMSE scheme by a small amount of prior knowledge.

Index Terms

New radio, OFDM, multiple antennas, channel estimation, demodulation reference signal, minimum mean square error.

I. INTRODUCTION

As the most well-known multicarrier modulation, orthogonal frequency division multiplexing (OFDM) has been adopted in various wireless communication standards [1]–[4], due to the ease

D. Kong is with the School of Electronic and Electrical Engineering, Wuhan Textile University, Wuhan, 430074, China (e-mail: djkou@wtu.edu.cn).

X.-G. Xia with the Department of Electrical and Computer Engineering, University of Delaware, Newark, DE 19716, USA (e-mail: xxia@ee.udel.edu)

P. Liu (Corresponding author) is with the School of Information Engineering, Wuhan University of Technology, Wuhan 430070, China (e-mail: pei.liu@ieec.org).

Q. Zhu is with the School of Information Engineering, Nanchang University, Nanchang 330031, China (e-mail: zhuqibiao@ncu.edu.cn).

of implementation and the ability to fight against multi-path fading channels [5], [6]. Recently, it has been agreed by the third generation partnership project (3GPP) that, OFDM is employed as the physical-layer technique for both of the downlink and uplink in new radio (NR) [7], [8] for the fifth-generation mobile communications (5G), and demodulation reference signal (DMRS) with multiple ports are designed to achieve the channel estimation as well as the equalization on data symbols.

In NR, two types of DRMS are adopted, i.e., Type 1 and Type 2 [7]. In Type 1, a pair of adjacent subcarriers distinguish two DMRS ports by employing the orthogonal cover code (OCC) and 2 of each 6 subcarriers are selected for the two DMRS ports. In Type 2, half of the frequency subcarriers are selected and cyclic shift phases are adopted to distinguish two DMRS ports. In this paper, we only focus on the channel estimation based on DMRS of Type 2. In general, the channel estimation can be achieved by the classical discrete Fourier transform (DFT) scheme [9]–[11] since channels for the two ports of DMRS can be separated in the time domain by the DFT operation. Since the two DMRS ports in NR are equivalent to orthogonal by OCC, the OCC-based method in [12] can be employed to separate the two DMRS ports, based on the assumption that channel frequency responses at adjacent subcarriers are equal. In [13], a robust channel estimator was presented for OFDM systems and it was shown that the minimum mean square error (MMSE) estimator is insensitive to the channel statistics. Furthermore, in [14], it was demonstrated that, the MMSE estimator is robust to correlation matrix mismatch for the multi-user scenario, which makes the MMSE channel estimation more practical. To the best of our knowledge, little is known about utilizing the MMSE metric for the channel estimation of two-port DMRS in NR in the open literature.

In this paper, we propose a new approach for the two-port channel estimation in NR, based on the MMSE metric. Firstly, we propose an MMSE with full priori knowledge (F-MMSE) scheme to achieve the channel estimation of two-port DMRS in NR. Then, we present an MMSE with partial priori knowledge (P-MMSE) scheme when the two ports are assigned to different users and the full priori knowledge of two ports is not easy to obtain for one user. Finally, theoretical analysis and numerical simulations are carried out to validate the performance of the proposed schemes. They show that the proposed two schemes can achieve high quality channel estimation. They also show that the proposed two schemes perform far better than the classical DFT scheme. More importantly, the P-MMSE scheme approaches to the same performance of the F-MMSE scheme with a little priori knowledge.

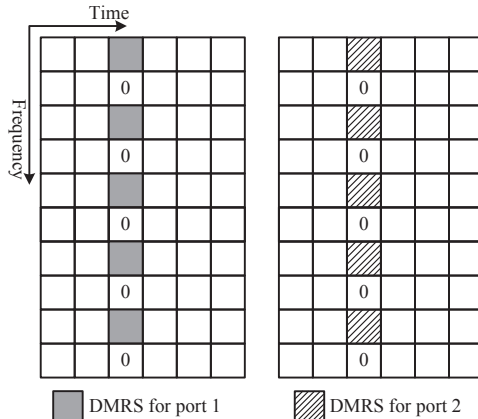


Fig. 1. Frame structure of two DMRS ports in NR

The remainder of this paper is organized as follows. In Section II, the system model and two-port of DMRS in NR are presented briefly, as well as the classical DFT-based channel estimation method and. In Section III, the two-port MMSE channel estimation methods are proposed. Simulation results are given in Section IV and this paper is concluded in Section V.

Notation: Lower-case and upper-case boldface letters denote vectors and matrices, respectively. \mathbf{I}_P denotes a $P \times P$ identity matrix. $(\cdot)^\dagger$, $(\cdot)^T$, and $(\cdot)^{-1}$ denote the Hermitian transpose, transpose, and inverse operations, respectively. The expectation operation is $\mathbb{E}\{\cdot\}$. $\text{diag}(\mathbf{a})$ denotes a diagonal matrix where the main diagonal entries are the elements of vector \mathbf{a} . Finally, $\|\cdot\|_2$ denotes the 2-norm of a vector.

II. CONVENTIONAL CHANNEL ESTIMATION SCHEMES

A. System Model

We consider an OFDM system with M subcarriers, equipped with two transmitting antennas and two receiving antennas. Assume that $2P < M$ subcarriers are assigned to one user, two ports of DMRS are as shown in Figure 1, which share the same time frequency resources. Assume $x_p = a_{2p,q}$ is the pilot of DMRS with the transmitting power of 1, where $p = 0, 1, \dots, P-1$ is the frequency index and q is the time index, Moreover, $a_{2p+1,q}$ is usually set to zero unless it is used to support more DMRS ports. Hence, in this paper, $a_{2p+1,q}$ is set to zero. If x_p is the pilot symbol of the first DMRS port, the pilot symbol of the second DMRS port would be $x_p e^{j2\pi \frac{p\Delta_{cs}}{P}}$ [7], where Δ_{cs} is the cyclic shift and it is equal $\frac{P}{2}$ for the orthogonality of two DMRS ports.

Then, the demodulation of the r th receiving antenna can be written as

$$y_p^r = h_p^{1r} x_p + h_p^{2r} x_p e^{j2\pi \frac{p\Delta_{cs}}{P}} + \eta_p^r, \quad (1)$$

where $r = 0$ or 1 , h_p^{tr} is the channel frequency response for p th pilot, between the t th transmitting antenna and the r th receiving antenna, and η_p^r is the additive white Gaussian noise with mean zero and variance σ^2 [15], [16].

For simplicity, the matrix form of (1) is obtained as

$$\mathbf{y}_r = \mathbf{X}\mathbf{h}_{1r} + \mathbf{X}\mathbf{C}\mathbf{h}_{2r} + \boldsymbol{\eta}_r, \quad (2)$$

where $\mathbf{y}_r = [y_0^r, y_1^r, \dots, y_{P-1}^r]^T$, $\mathbf{h}_{tr} = [h_0^{tr}, h_1^{tr}, \dots, h_{P-1}^{tr}]^T$, $\boldsymbol{\eta}_r = [\eta_0^r, \eta_1^r, \dots, \eta_{P-1}^r]^T$, and $\mathbf{X} = \text{diag}(x_0, \dots, x_p, \dots, x_{P-1})$. Also, \mathbf{C} is a diagonal matrix and its p th diagonal element is $e^{j2\pi \frac{p\Delta_{cs}}{P}}$.

Note that, \mathbf{X} is a diagonal and reversible matrix. Then, the two-port DMRS-based channel estimation model can be obtained [11], as

$$\hat{\mathbf{h}} = \mathbf{X}^{-1}\mathbf{y}_r = \mathbf{h}_{1r} + \mathbf{C}\mathbf{h}_{2r} + \mathbf{X}^{-1}\boldsymbol{\eta}_r, \quad (3)$$

where \mathbf{X}^{-1} is the inverse matrix of \mathbf{X} .

In this paper, we assume that the two DMRS ports are assigned to different users. For downlink transmission, each user has to perform channel estimation independently.

B. DFT-based Channel Estimation

In this subsection, the DFT-based scheme is briefly presented to achieve the channel estimation of two-port DMRS. Firstly, a P -point inverse DFT (IDFT) operation is performed on $\hat{\mathbf{h}}$, and it is obtained as

$$\underline{\mathbf{h}} = \mathbf{F}\hat{\mathbf{h}} = \underline{\mathbf{h}}_{1r} + \underline{\mathbf{h}}_{2r} \left(\frac{P}{2} \right) + \boldsymbol{\xi}_r, \quad (4)$$

where \mathbf{F} is the IDFT matrix with dimension of $P \times P$, whose element at the position (p, q) is $\frac{1}{\sqrt{P}} e^{j2\pi \frac{pq}{P}}$, and $\boldsymbol{\xi}_r = \mathbf{F}\mathbf{X}^{-1}\boldsymbol{\eta}_r$. Also, $\underline{\mathbf{h}}_{tr}$ is the channel impulse response between the t th transmitting antenna and the r th receiving antenna, and $\underline{\mathbf{h}}_{2r} \left(\frac{P}{2} \right)$ is a cyclic shift vector of $\underline{\mathbf{h}}_{2r}$ with a shift $\frac{P}{2}$. Note that, the number of subcarriers in OFDM should be at least twice larger than the channel length.

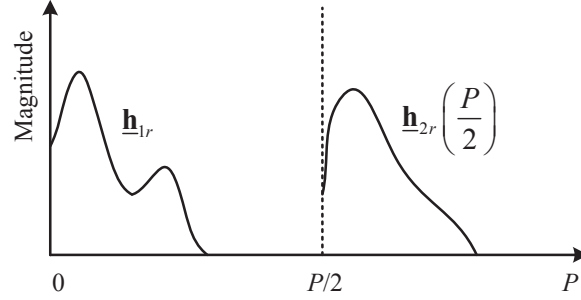


Fig. 2. Separation of channels in the DFT-based channel estimation.

From (4), it can be observed that, the channel impulse responses $\underline{\mathbf{h}}_{1r}$ and $\underline{\mathbf{h}}_{2r}$ are separated by $\frac{P}{2}$ in the time domain as shown in Figure 2, and the time-domain channel estimation can be performed by the following function,

$$g(p) = \begin{cases} 1, & 0 \leq p < \frac{P}{2} - 1, \\ 0, & \frac{P}{2} \leq p < P - 1, \end{cases} \quad (5)$$

Denote a $P \times P$ diagonal matrix \mathbf{G} with the diagonal element $g(p)$. Then, the channel estimation of $\underline{\mathbf{h}}_{1r}$ can be obtained as

$$\hat{\underline{\mathbf{h}}}_{1r} = \mathbf{G}\hat{\underline{\mathbf{h}}}. \quad (6)$$

Then, the channel frequency responses can be obtained by a P -point DFT operation

$$\hat{\mathbf{h}}_{1r}^{\text{DFT}} = \mathbf{G}\hat{\underline{\mathbf{h}}}_{1r}. \quad (7)$$

As for \mathbf{h}_{2r} , the channel estimation can be performed by the same principle.

C. OCC-based MMSE

It is noted that, when $\Delta_{cs} = P/2$ with an even number P for simplicity, the two DMRS ports, x_{2p} , x_{2p+1} for the first port and x_{2p} , $-x_{2p+1}$ for the second port with $p = 0, 1, \dots, P/2 - 1$, can be separated by the orthogonal cover code (OCC), i.e., $[1, 1]$ and $[1, -1]$. In this subsection, the OCC-based MMSE channel estimation scheme is presented for the two DMRS ports.

Firstly, equation (1) can be rewritten as

$$\begin{cases} y_{2p}^r/x_{2p} = h_{2p}^{1r} + h_{2p}^{2r} + \eta_{2p}^r/x_{2p}, \\ y_{2p+1}^r/x_{2p+1} = h_{2p+1}^{1r} - h_{2p+1}^{2r} + \eta_{2p+1}^r/x_{2p+1}, \quad p = 0, 1, \dots, P/2 - 1. \end{cases} \quad (8)$$

Note that, x_p has transmitting power of 1, therefore, noise η_p^r/x_p satisfies the Gaussian distribution with mean 0 and σ^2 .

Assume that channel frequency responses, h_{2p}^{tr} and h_{2p+1}^{tr} are equal, i.e., $h_{2p}^{tr} = h_{2p+1}^{tr}$. Then, equation (8) can be rewritten as

$$\begin{cases} y_{2p}^r/x_{2p} = h_{2p}^{1r} + h_{2p}^{2r} + \eta_{2p}^r/x_{2p}, \\ y_{2p+1}^r/x_{2p+1} = h_{2p}^{1r} - h_{2p}^{2r} + \eta_{2p+1}^r/x_{2p+1}, \quad p = 0, 1, \dots, P/2 - 1. \end{cases} \quad (9)$$

Denote $\bar{y}_p^r = y_p^r/x_p$ and $\bar{\eta}_p^r = \eta_p^r/x_p$. Then, each user can perform the channel estimation independently as

$$\begin{cases} \hat{h}_{2p}^{1r} = \frac{\bar{y}_{2p}^r + \bar{y}_{2p+1}^r}{2} = h_{2p}^{1r} + \frac{\bar{\eta}_{2p}^r + \bar{\eta}_{2p+1}^r}{2}, \\ \hat{h}_{2p}^{2r} = \frac{\bar{y}_{2p}^r - \bar{y}_{2p+1}^r}{2} = h_{2p}^{2r} + \frac{\bar{\eta}_{2p}^r - \bar{\eta}_{2p+1}^r}{2}, \quad p = 0, 1, \dots, P/2 - 1. \end{cases} \quad (10)$$

Then, the channel estimation can be improved by the MMSE criteria, which can be obtained as

$$\hat{\mathbf{h}}_{tr}^{\text{OCC-MMSE}} = \mathbf{R}_{tr} (\mathbf{R}_{tr} + \sigma^2 \mathbf{I}_{P/2})^{-1} \hat{\mathbf{h}}_{tr}. \quad (11)$$

where $\hat{\mathbf{h}}_{tr} = [\hat{h}_0^{tr}, \hat{h}_2^{tr}, \dots, \hat{h}_{P-2}^{tr}]^T$. \mathbf{R}_{tr} is the auto-covariances of $\mathbf{h}_{tr} = [h_0^{tr}, h_2^{tr}, \dots, h_{P-2}^{tr}]^T$.

It is worthwhile noting that, the OCC-based MMSE is based the assumption $h_{2p}^{tr} = h_{2p+1}^{tr}$, which indicates a performance loss of channel estimation under highly frequency selective channels. Especially, for the two DMRS ports as presented in Figure. 1, the pilot symbols locate at every two subcarriers. Therefore, the channel frequency responses at m -th and $(m + 2)$ -th subcarriers are required to be equal in the classical OCC-based MMSE scheme.

III. PROPOSED SCHEMES FOR TWO-PORT DMRS

In this section, we firstly present the F-MMSE scheme based on the full priori knowledge of the two ports for channel estimation in NR. When the two ports are assigned to different users

and the full priori knowledge of two ports is difficult to obtain for one user. Then, the P-MMSE scheme is presented for two-port channel estimation, based the partial knowledge of only one port. For simplicity, the channel estimation of \mathbf{h}_{1r} is only presented in detail in this paper and the estimation of \mathbf{h}_{2r} can be done in the same way.

A. F-MMSE Channel Estimation

For the channel estimation model in (3), \mathbf{h}_{1r} is the random vector of parameters to be estimated. Then, the F-MMSE channel estimation of \mathbf{h}_{1r} can be obtained by minimizing the mean square error (MSE), defined as

$$\text{MSE} = \mathbb{E} \left\{ \left\| \mathbf{h}_{1r} - \hat{\mathbf{h}}_{1r} \right\|_2^2 \right\}, \quad (12)$$

where $\hat{\mathbf{h}}_{1r}$ is an estimate of \mathbf{h}_{1r} . Subsequently, the F-MMSE channel estimation of \mathbf{h}_{1r} can be obtained by minimizing the MSE

$$\hat{\mathbf{h}}_{1r}^{\text{F-MMSE}} = \mathbf{R}_{\hat{\mathbf{h}}\mathbf{h}_{1r}} \mathbf{R}_{\hat{\mathbf{h}}\hat{\mathbf{h}}}^{-1} \hat{\mathbf{h}}, \quad (13)$$

where $\mathbf{R}_{\hat{\mathbf{h}}\mathbf{h}_{1r}}$ is the cross covariance matrix between $\hat{\mathbf{h}}$ and \mathbf{h}_{1r} . Further, $\mathbf{R}_{\hat{\mathbf{h}}\hat{\mathbf{h}}}$ is the auto covariance matrix of $\hat{\mathbf{h}}$. $\mathbf{R}_{\hat{\mathbf{h}}\mathbf{h}_{1r}}$ and $\mathbf{R}_{\hat{\mathbf{h}}\hat{\mathbf{h}}}^{-1}$ are obtained as

$$\mathbf{R}_{\hat{\mathbf{h}}\mathbf{h}_{1r}} = \mathbb{E} \left\{ \mathbf{h}_{1r} \hat{\mathbf{h}}^\dagger \right\} = \mathbf{R}_{1r}, \quad (14)$$

$$\mathbf{R}_{\hat{\mathbf{h}}\hat{\mathbf{h}}} = \mathbb{E} \left\{ \hat{\mathbf{h}} \hat{\mathbf{h}}^\dagger \right\} = \mathbf{R}_{1r} + \mathbf{C} \mathbf{R}_{2r} \mathbf{C}^\dagger + \sigma^2 \mathbf{I}_P, \quad (15)$$

respectively, where \mathbf{I}_P is an identity matrix with dimension of P . \mathbf{R}_{1r} and \mathbf{R}_{2r} are auto-covariances of \mathbf{h}_{1r} and \mathbf{h}_{2r} . Therefore, based on the priori knowledge \mathbf{R}_{1r} and \mathbf{R}_{2r} , the F-MMSE can be obtained as

$$\hat{\mathbf{h}}_{1r}^{\text{F-MMSE}} = \mathbf{R}_{1r} (\mathbf{R}_{1r} + \mathbf{C} \mathbf{R}_{2r} \mathbf{C}^\dagger + \sigma^2 \mathbf{I}_P)^{-1} \hat{\mathbf{h}}. \quad (16)$$

As a remark, when only one of the two DMRS ports is used, i.e., no signal is transmitted via the second DMRS port, the optimal MMSE channel estimation of \mathbf{h}_{1r} is

$$\hat{\mathbf{h}}_{1r}^{\circ} = \mathbf{R}_{1r} (\mathbf{R}_{1r} + \sigma^2 \mathbf{I}_P)^{-1} \hat{\mathbf{h}}. \quad (17)$$

Note that although the above F-MMSE, i.e., MMSE, is straightforward, it helps us to develop a more practical estimator below.

B. P-MMSE Channel Estimation

For (16), one has to get the priori knowledge of both the two DRMS ports, i.e., \mathbf{R}_{1r} and \mathbf{R}_{2r} . However, when the two DMRS ports are assigned to different users, one user performing the channel estimation does not know the priori knowledge of another DMRS port and that whether another DMRS port is used or not. In our proposed P-MMSE scheme, we replace \mathbf{R}_{2r} by \mathbf{R}_{1r} and the channel estimation is written as

$$\hat{\mathbf{h}}_{1r}^{\text{P-MMSE}} = \mathbf{R}_{1r} (\mathbf{R}_{1r} + \mathbf{C}\mathbf{R}_{1r}\mathbf{C}^\dagger + \sigma^2\mathbf{I}_P)^{-1} \hat{\mathbf{h}}. \quad (18)$$

To show the validity of the proposed P-MMSE scheme, the theoretical analysis is presented in the following. Firstly, the frequency-domain estimation in (18) is converted into the time domain as

$$\underline{\hat{\mathbf{h}}}_{1r}^{\text{P-MMSE}} = \mathbf{F}\hat{\mathbf{h}}_{1r}^{\text{P-MMSE}} = \mathbf{F}\mathbf{R}_{1r} (\mathbf{R}_{1r} + \mathbf{C}\mathbf{R}_{1r}\mathbf{C}^\dagger + \sigma^2\mathbf{I}_P)^{-1} \mathbf{F}^\dagger \hat{\mathbf{h}} \quad (19)$$

Substituting (4) into (19), we have

$$\begin{aligned} \underline{\hat{\mathbf{h}}}_{1r}^{\text{P-MMSE}} &= \mathbf{F}\mathbf{R}_{1r} (\mathbf{R}_{1r} + \mathbf{C}\mathbf{R}_{1r}\mathbf{C}^\dagger + \sigma^2\mathbf{I}_P)^{-1} \mathbf{F}^\dagger \left(\underline{\mathbf{h}}_{1r} + \underline{\mathbf{h}}_{2r} \left(\frac{P}{2} \right) + \boldsymbol{\xi}_r \right) \\ &= \boldsymbol{\Phi}_{1r}^{\text{P-MMSE}} \left(\underline{\mathbf{h}}_{1r} + \underline{\mathbf{h}}_{2r} \left(\frac{P}{2} \right) \right) + \boldsymbol{\Phi}_{1r}^{\text{P-MMSE}} \boldsymbol{\xi}_r, \end{aligned} \quad (20)$$

where $\boldsymbol{\Phi}_{1r}^{\text{P-MMSE}} = \mathbf{F}\mathbf{R}_{1r} (\mathbf{R}_{1r} + \mathbf{C}\mathbf{R}_{1r}\mathbf{C}^\dagger + \sigma^2\mathbf{I}_P)^{-1} \mathbf{F}^\dagger$. Note that the coefficient matrix of the proposed F-MMSE scheme is $\boldsymbol{\Phi}_{1r}^{\text{F-MMSE}} = \mathbf{F}\mathbf{R}_{1r} (\mathbf{R}_{1r} + \mathbf{C}\mathbf{R}_{2r}\mathbf{C}^\dagger + \sigma^2\mathbf{I}_P)^{-1} \mathbf{F}^\dagger$.

It is observed that from (20), the estimation $\underline{\hat{\mathbf{h}}}_{1r}^{\text{P-MMSE}}$ is a linear combination of $\underline{\mathbf{h}}_{1r}$ and $\underline{\mathbf{h}}_{2r} \left(\frac{P}{2} \right)$ by the P-MMSE coefficient $\boldsymbol{\Phi}_{1r}^{\text{P-MMSE}}$. It can be easily seen that, the values of the channel estimation mainly depend on the diagonal coefficients of the matrix $\boldsymbol{\Phi}_{1r}^{\text{P-MMSE}}$. As a result, Figure 3 depicts the magnitudes of the diagonal elements of the P-MMSE and F-MMSE coefficient matrices, in which $P = 120$ and $M = 2048$. In addition, a random channel model is adopted with 40 sample-spaced independent Rayleigh fading paths, which exhibit an exponential power delay profile [17] as $\alpha(l) = e^{\beta l}$, where $l = 0, 1, \dots, 39$, $\beta = -0.0005$ for the first DMRS port and $\beta = -0.05$ for the second DMRS port, i.e., $\beta = -0.0005$ is for the channels \mathbf{h}_{11} and \mathbf{h}_{12} , and $\beta = -0.05$ is for the channels \mathbf{h}_{21} and \mathbf{h}_{22} . The different β in channels lead to the different channel covariance matrices. From the simulation results, the magnitude of the diagonal element of the P-MMSE coefficient matrix is accordance to that of F-MMSE despite

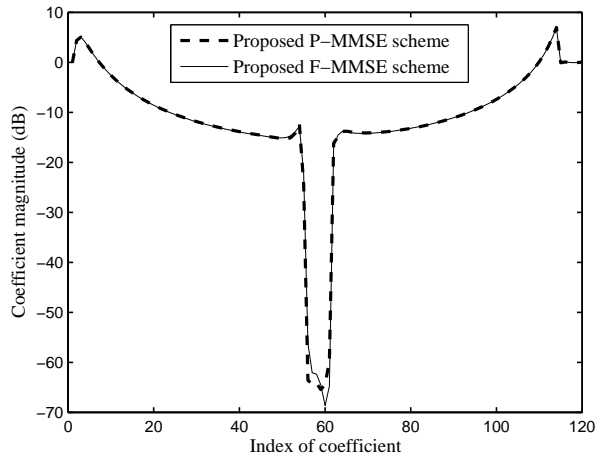


Fig. 3. Magnitudes of the diagonal elements of the P-MMSE and F-MMSE coefficient matrices, i.e., $\Phi_{1r}^{\text{P-MMSE}}$ and $\Phi_{1r}^{\text{F-MMSE}}$, SNR = 30 dB.

of the large difference of the attenuation factor β , exhibiting insensitive to channel covariance matrices. Furthermore, it can be observed that, the P-MMSE coefficients have very small values at the points around $\frac{P}{2}$, which indicates that, for the channel estimation of \mathbf{h}_{1r} the interference from $\mathbf{h}_{2r}(\frac{P}{2})$ is greatly suppressed since channel coefficients of $\mathbf{h}_{2r}(\frac{P}{2})$ have valid values at round $\frac{P}{2}$ as you can see Figure 2. As a remark, it is worthwhile to note that, the P-MMSE coefficients have valid values at round both of 0 and P . The reason is that when the subcarrier number of users is less than the system subcarrier, i.e., $P < M$, the energy of channels coefficients is leaked at the points around P due to the Gibbs phenomenon [18].

C. MSE Analysis

In this subsection, MSE of the proposed F-MMSE and P-MMSE estimators are analyzed. Without loss of generality, only MSE with respect to \mathbf{h}_{1r} is considered.

Firstly, MSE of the proposed F-MMSE can be obtained by

$$\text{MSE}_F = \text{Tr} \left\{ \mathbb{E} \left[\left(\hat{\mathbf{h}}_{1r}^{\text{F-MMSE}} - \mathbf{h}_{1r} \right) \left(\hat{\mathbf{h}}_{1r}^{\text{F-MMSE}} - \mathbf{h}_{1r} \right)^\dagger \right] \right\}, \quad (21)$$

where $\text{Tr}\{\cdot\}$ denotes the trace operation.

It should be pointed out that, the channels \mathbf{h}_{1r} , \mathbf{h}_{2r} , and noise $\boldsymbol{\eta}_r$ are independent. Therefore, it can be obtained

$$\mathbb{E}[\mathbf{h}_{1r} \mathbf{h}_{2r}^\dagger] = 0, \quad (22)$$

$$\mathbb{E}[\mathbf{h}_{1r}\boldsymbol{\eta}_r^\dagger] = 0, \quad (23)$$

$$\mathbb{E}[\mathbf{h}_{2r}\boldsymbol{\eta}_r^\dagger] = 0. \quad (24)$$

For simplicity of presentation, we denote $\mathbf{R}_{1r} (\mathbf{R}_{1r} + \mathbf{C}\mathbf{R}_{2r}\mathbf{C}^\dagger + \sigma^2\mathbf{I}_P)^{-1}$ in equation (16) as \mathbf{A} . Then, by substituting equations (3) and (16) into (21), the MSE of the proposed F-MMSE estimator is easily obtained

$$\text{MSE}_F = \text{Tr} \{ \mathbf{A}\mathbf{R}_{1r}\mathbf{A}^\dagger + \mathbf{A}\mathbf{C}\mathbf{R}_{2r}\mathbf{C}^\dagger\mathbf{A}^\dagger + \mathbf{A}\mathbf{A}^\dagger\sigma^2 - \mathbf{A}\mathbf{R}_{1r} - \mathbf{R}_{1r}\mathbf{A}^\dagger + \mathbf{R}_{1r} \}. \quad (25)$$

Similarity, we denote $\mathbf{R}_{1r} (\mathbf{R}_{1r} + \mathbf{C}\mathbf{R}_{1r}\mathbf{C}^\dagger + \sigma^2\mathbf{I}_P)^{-1}$ in equation (18) as \mathbf{B} , and the MSE of the proposed P-MMSE estimator can be obtained

$$\text{MSE}_P = \text{Tr} \{ \mathbf{B}\mathbf{R}_{1r}\mathbf{B}^\dagger + \mathbf{B}\mathbf{C}\mathbf{R}_{2r}\mathbf{C}^\dagger\mathbf{B}^\dagger + \mathbf{B}\mathbf{B}^\dagger\sigma^2 - \mathbf{B}\mathbf{R}_{1r} - \mathbf{R}_{1r}\mathbf{B}^\dagger + \mathbf{R}_{1r} \}. \quad (26)$$

It can be observed that, MSE of F-MMSE and P-MMSE estimators depend on the MMSE coefficients, i.e., \mathbf{A} and \mathbf{B} , respectively. As presented in Subsection III-B, the MMSE coefficient is insensitive to channel covariance mismatching. As a result, the coefficients of \mathbf{A} is close to the coefficients of \mathbf{B} , which indicates the proposed P-MMSE estimator has a similar MSE performance with the F-MMSE estimator.

IV. SIMULATION RESULTS

In this section, numerical simulations are carried out to show the validity of the proposed schemes in a 2×2 multiple-antenna OFDM system with $P = 120$ and $M = 2048$, in which the system sampling rate is 30.72MHz. In simulations, quadrature phase shift keying (QPSK) modulation and no channel coding scheme are considered. In addition, the length of cyclic prefix is 144 samples.

Figure 4 shows the channel magnitude responses of the proposed P-MMSE and F-MMSE schemes to evaluate the validity of channel estimation, in which the channel models in Subsection 3.2 are adopted and signal-to-noise ratio (SNR) is set to 30 dB to make the noise small enough. It is easily observed that, the channel estimations of the proposed P-MMSE and F-MMSE schemes are accordance to the perfect channel \mathbf{h}_{11} , without significant interference. Note that, the P-MMSE scheme approaches to the same performance of the F-MMSE scheme with a little priori knowledge.

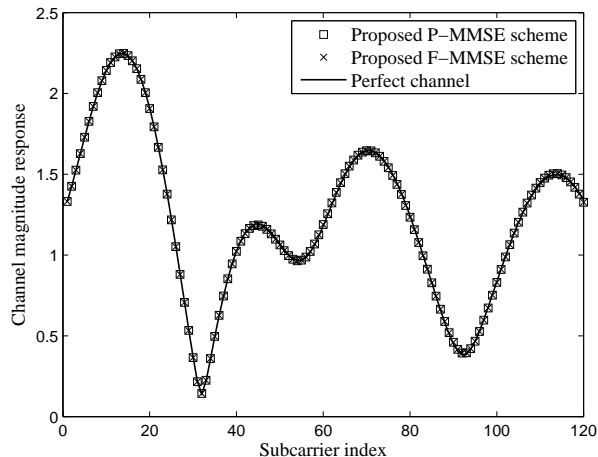


Fig. 4. Channel magnitude responses of $\hat{\mathbf{h}}_{11}^{\text{P-MMSE}}$, $\hat{\mathbf{h}}_{11}^{\text{F-MMSE}}$ and the true channel \mathbf{h}_{11} , SNR = 30 dB.

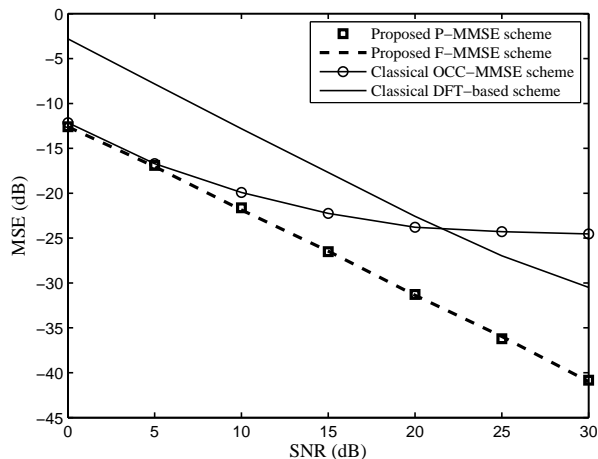


Fig. 5. MSE comparison of the proposed P-MMSE scheme, the proposed F-MMSE scheme, and the classical DFT-based scheme under channels with exponential power delay profiles.

Figure 5 and Figure 6 depict the mean square error (MSE) and bit error ratio (BER) performances of the proposed P-MMSE and F-MMSE schemes, respectively. In simulations, the channel models in Subsection 3.2 are adopted. For comparison, we also give the performances of the classical DFT-based scheme and the OCC-based MMSE scheme. From simulation results, the proposed P-MMSE and F-MMSE schemes exhibit large gains in terms of MSE and BER compared with the classical DFT-based scheme, since the classical DFT-based scheme does not require the priori knowledge of channel covariance matrix. It is also observed that, compared with the proposed P-MMSE and F-MMSE schemes, the classical OCC-based MMSE can achieve

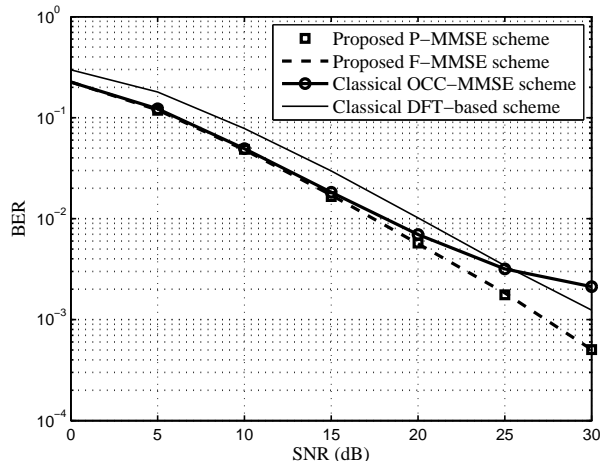


Fig. 6. BER comparison of the proposed P-MMSE scheme, the proposed F-MMSE scheme, and the classical DFT-based scheme under channels with exponential power delay profiles.

similar MSE and BER performances at low SNR region and suffers from obvious loss at high SNR region. The reason is that the classical OCC-based MMSE is based on the assumption that the channel frequency responses at adjacent subcarrier are equal, which indicates performance loss under high frequency selective channels. Note that, as depicted in Figure 1, pilot symbols of the two DMRS ports locate at every two subcarriers, therefore, the channel frequency responses at m -th and $(m + 2)$ -th subcarriers are required to be equal in the classical OCC-based MMSE scheme. On the other hand, the proposed F-MMSE scheme can achieve the optimal channel estimation performance, with the full priori knowledge of both DMRS ports, i.e., \mathbf{R}_{1r} and \mathbf{R}_{2r} . When the two DMRS ports are assigned to two different users, the full priori knowledge is not easy to obtain for one user. The proposed P-MMSE only requires the priori knowledge of one port and can achieve the similar performance compared with the proposed F-MMSE, despite the large difference of the attenuation factors of exponential power delay profiles.

To evaluate the proposed schemes under more practical channel models, tapped delay line (TDL) models [19] released by 3GPP are also used in simulations. Note that, the two DMRS ports are assigned to different channel models. Specifically, the first DMRS port is with TDL-A and the second DMRS port is with TDL-C, in which TDL-A and TDL-C exhibit different delay spreads and power delay profiles [19]. Figure 7 shows BER comparison of the proposed P-MMSE scheme and F-MMSE scheme under the TDL channels. From simulation results, the proposed P-MMSE achieves the similar BER performance compared with the optimal F-MMSE,

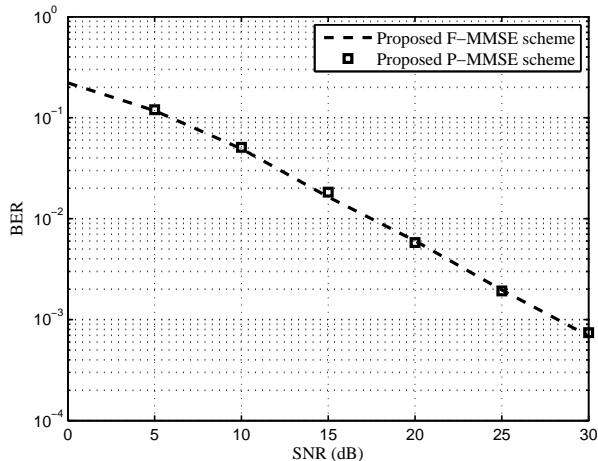


Fig. 7. BER comparison of the proposed P-MMSE scheme and the proposed F-MMSE scheme, under the TDL channels.

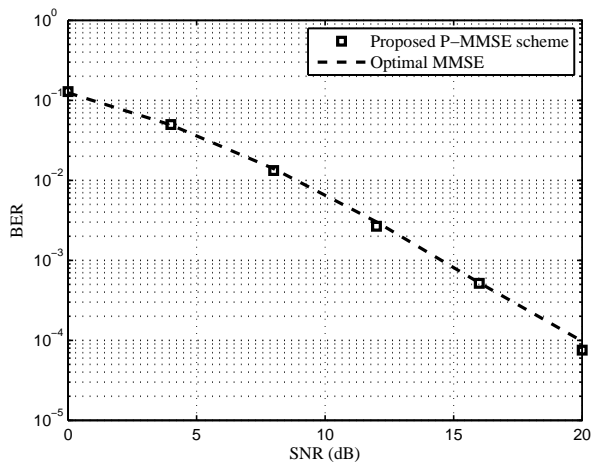


Fig. 8. BER performance of the proposed P-MMSE scheme under the TDL channels when only one of the two DMRS ports is used.

which validates the effectiveness of the proposed P-MMSE scheme.

When only one of the two DMRS ports is used, the 2×2 multiple-antenna OFDM system becomes a 1×2 multiple-antenna system. In this case, the optimal MMSE channel estimation will be equation (17). However, for one user with the first DMRS port, it is difficult to obtain the priori knowledge on whether another DMRS port is used or not. Figure 8 shows the BER performance of the proposed P-MMSE scheme under the TDL channels when only one of the two DMRS ports is used. For comparison, the performance of the optimal MMSE as (17) is also given. From simulation results, the proposed P-MMSE achieves a similar BER performance

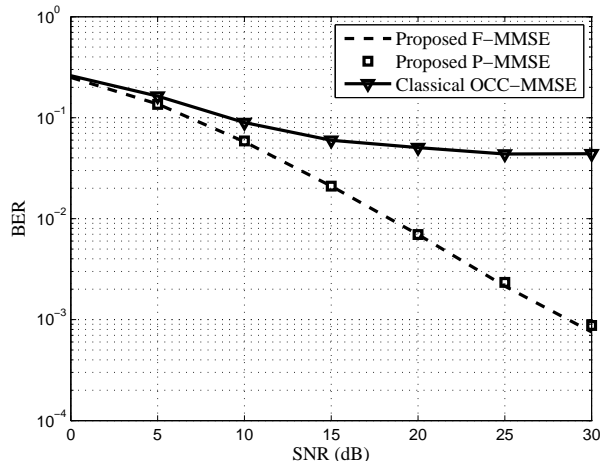


Fig. 9. BER performance of the proposed P-MMSE scheme under TDL-C and the channel with equal-power delay profiles.

compared with the optimal MMSE.

Then, the first DMRS port is with the TDL-C channel and the second DMRS port is with the channel with equal-power power delay profiles and maximum channel delay spread $9.65860\mu s$. Figure 9 shows BER comparison of the proposed P-MMSE scheme and F-MMSE scheme under the TDL channel and the channel with equal-power delay profiles [14]. From simulation results, the proposed P-MMSE achieves the similar BER performance compared with the optimal F-MMSE, which validates the effectiveness of the proposed P-MMSE scheme. Besides, the classical OCC-based MMSE suffers from obvious performance loss. The reason is that the classical OCC-based MMSE is based on the assumption that the channel frequency responses at adjacent subcarrier are equal, which is not satisfied well under the high frequency selective channels.

V. CONCLUSION

In this paper, we firstly proposed the F-MMSE scheme to achieve the channel estimation of two-port DMRS in NR, which requires the full priori knowledge of the channel covariance matrix of two ports. Then, we presented the P-MMSE scheme with the priori knowledge of only one DMRS port. Finally, theoretical analysis and numerical simulations showed that the proposed two schemes achieve satisfactory channel estimation performance. Also, the proposed P-MMSE scheme is insensitive to the difference of channel covariance matrices of the two DMRS ports, and can achieve the similar performance compared with the F-MMSE scheme.

Both of the proposed P-MMSE and F-MMSE schemes have large gains in terms of MSE and BER compared with the classical DFT-based scheme.

REFERENCES

- [1] W. Ma, C. Qi, and G. Y. Li, "High-resolution channel estimation for frequency-selective mmWave massive MIMO systems," *IEEE Trans. Wireless Commun.*, vol. 19, no. 5, pp. 3517-3529, May 2020.
- [2] J. Fan, Q. Yin, and W. Wang, "Pilot-aided channel estimation for CDD-OFDM systems," *Sci. China Inf. Sci.*, vol. 53, no. 2, pp. 379-389, Feb 2010.
- [3] A. Ghosh, R. Ratasuk, B. Mondal, N. Mangalvedhe, and T. Thomas, "LTE-Advanced: next-generation wireless broadband technology," *IEEE Wireless Commun.*, vol. 17, no. 3, pp. 10-22, Jun. 2010.
- [4] Y. Li, X. Xu, D. Zhang, Z. Zhang, and K. Long, "Optimal pilots design for frequency offsets and channel estimation in OFDM modulated single frequency networks," *Sci. China Inf. Sci.*, vol. 57, Apr. 2014.
- [5] M. El-Absi, S. Galih, M. Hoffmann, M. El-Hadidy, and T. Kaiser, "Antenna selection for reliable MIMO-OFDM interference alignment systems: measurement-based evaluation," *IEEE Trans. Veh. Technol.*, vol. 65, no. 5, pp. 2965-2977, May. 2016.
- [6] S. Nagaraj, "Pre-DFT combining for coded OFDM," *IEEE Trans. Veh. Technol.*, vol. 58, no. 9, pp. 5305-5309, Nov. 2009.
- [7] 3GPP, "NR; Physical channels and modulation (Release 15)," v15.1.0, TS 38.211, 2018. [Online]. Available: http://www.3gpp.org/ftp/Specs/archive/38_series/38.211/38211-f10.zip
- [8] C. B. Barneto, T. Riihonen, M. Turunen, L. Anttila, M. Fleischer, K. Stadius, J. Ryyänen, and M. Valkama, "Full-duplex OFDM radar with LTE and 5G NR waveforms: challenges, solutions, and measurements," *IEEE Trans. Microw. Theory Techn.*, vol. 67, no. 10, pp. 4042-4054, Aug. 2019.
- [9] M. Jiang, G. Yue, N. Prasad, and S. Rangarajan. "Enhanced DFT-based channel estimation for LTE uplink," in *Proc. IEEE VTC Spring*, May 2012.
- [10] X. Li, X. Jing, S. Sun, H. Huang, and Y. Lu. "An improved DFT-based channel estimation method for OFDM system," in *Proc. IET CCT*, Nov. 2013, pp. 550-554.
- [11] J. Zhang, and L. Huang. "An improved DFT-based channel estimation algorithm for MIMO-OFDM systems," in *Proc. CECNET*, Apr. 2011, pp. 3929-3932.
- [12] S. Sesia, I. Toufik, and M. Baker, *LTE-The UMTS Long Term Evolution: From Theory to Practice*. West Sussex, U.K.: John Wiley & Sons. Ltd., 2011.
- [13] Y. Li, L. J. Cimini, Jr., and N. R. Sollenberger, "Robust channel estimation for OFDM systems with rapid dispersive fading channels," *IEEE Trans. Commun.*, vol. 46, no. 7, pp. 902-915, Jul. 1998.
- [14] Y. Zhang, D. Wang, J. Wang, and X. You, "Channel estimation for massive MIMO-OFDM systems by tracking the joint angle-delay subspace," *IEEE Access*, vol. 4, pp. 10166-10179, 2016.
- [15] P. Liu, S. Jin, T. Jiang, Q. Zhang, and M. Matthaiou, "Pilot power allocation through user grouping in multi-cell massive MIMO systems," *IEEE Trans. Commun.*, vol. 65, no. 4, pp. 1561-1574, Apr. 2017.
- [16] D. Kong, X.-G. Xia, and T. Jiang, "An alamouti coded CP-FBMC-MIMO system with two transmit antennas," *Sci. China Inf. Sci.*, vol. 58, Oct. 2015.
- [17] D. Kong, D. Qu, and T. Jiang, "Time domain channel estimation for OQAM-OFDM systems: algorithms and performance bounds," *IEEE Trans. Signal Process.*, vol. 68, no. 2, pp. 322-330, Jan. 2014.
- [18] X. Hou, Z. Zhang, and H. Kayama, "DMRS design and channel estimation for LTE-advanced MIMO uplink," in *Proc. IEEE VTC Fall*, Sep. 2009.

- [19] 3GPP, “Technical specification group radio access network; study on channel model for frequencies from 0.5 to 100 GHz (Release 16),” v16.1.0, TS 38.901, 2019. [Online]. Available: https://www.3gpp.org/ftp/Specs/archive/38_series/38.901/38901-g10.zip